

# Unsupervised Anomaly Detection with Adversarial Mirrored AutoEncoders

Gowthami Somepalli<sup>1</sup>, Yexin Wu<sup>1</sup>, Yogesh Balaji<sup>1</sup>, Bhanukiran Vinzamuri<sup>2</sup>, Soheil Feizi<sup>1</sup>

<sup>1</sup>University of Maryland, College Park <sup>2</sup>IBM Research  
{gowthami,yogesh,soheil}@cs.umd.edu, ywu12319@terpmail.umd.edu, bhanu.vinzamuri@ibm.com

## Abstract

Deep neural networks have great predictive power when they are applied to the in-distribution test data, but they tend to predict incorrect outputs, highly confidently, for out-of-distribution (OOD) samples. Hence, it is of utmost importance to detect anomalous samples before deploying deep systems in the real world. The use of deep generative models for anomaly detection has shown great promise owing to their ability to learn proper representations of complex input data distributions. However, earlier studies have shown that generative models assign higher likelihoods to OOD samples compared to the data distribution they have been trained on. In this work, we propose Adversarial Mirrored AutoEncoder (AMA), a simple modification to Adversarial Autoencoder where we use a Mirrored Wasserstein loss in the Discriminator to enforce better semantic-level reconstruction. We also propose a new metric for anomaly quantification instead of a regular reconstruction-based metric which has been used in most of the recent generative model-based anomaly detection methods. We show that in an unsupervised setting, our model outperforms or matches recent anomaly detectors based on generative models over CIFAR-10 and MNIST on both in-distribution and OOD anomalies.

## Introduction

When we are deploying machine learning models in the real world, we have to ensure safety and reliability along with the performance. The models which perform exceptionally well on training data might fail when deployed in the wild. One of the reasons why this happens could be a distribution shift since data is dynamic while models are static. Recognizing anomalous samples in the landscape of constantly changing data is considered an important problem in AI safety (Amodei et al. 2016). Rather than predicting wrong values confidently when faced with such data, we should design the models to raise a flag so that a human operator can inspect. This flagging-step is of utmost importance in many real-life scenarios like self-driving or disease diagnosis. The task of identifying such novel or anomalous samples has been formalized as Anomaly Detection (AD). This problem has been studied for years under various names, like Novelty Detection, Out-of-Distribution Detection, Open set recognition, Uncertainty Estimation, and so on (Chandola, Banerjee, and Kumar 2009; Chalpathy and Chawla 2019).

Anomaly Detection is an umbrella term for such a problem, with many sub-cases. While most of the current anomaly detection models assume anomalies arise from a distribution very different from the training distribution (OOD anomalies), it might not always be the case. Anomalies could arise in-distribution as well (e.g. every class of CIFAR-10 may be considered anomalous with respect to other classes). We call these cases in-distribution or same-manifold anomalies. In this work, we strive to address both of these problems.

Most of the recent methods proposed to solve the OOD anomaly detection problem are of discriminative in nature, using confidence scores based on softmax probabilities (Hendrycks and Gimpel 2016; Liang, Li, and Srikant 2017; Vyas et al. 2018; Hsu et al. 2020; Hendrycks, Mazeika, and Dietterich 2018; Lee et al. 2018). In most of these methods, anomalies are not used in training the model itself, but they are used to tune the hyperparameters. While these methods perform exceptionally well when the class labels are available for the in-distribution training data, they cannot be used in unsupervised or semi-supervised scenarios where labels are missing for most of the classes. Generative modeling is a promising option for both unsupervised or semi-supervised Anomaly Detection.

A popular and intuitive way to use generative models in Anomaly Detection would be to train the model only on the normal samples and use the likelihood statistics to recognize the anomalies during test time. However, recent studies of using generative models for OOD detection (Choi, Jang, and Alemi 2018; Nalisnick et al. 2018; Ren et al. 2019) have found that deep generative models trained on a dataset (say CIFAR-10) are assigning higher likelihoods to some out-of-distribution (OOD) images (e.g. SVHN). This behaviour is persistent in a wide range of generative models such as Glow (Nalisnick et al. 2018; Choi, Jang, and Alemi 2018), PixelCNN, PixelCNN+ (Hendrycks, Mazeika, and Dietterich 2018; Shafaei, Schmidt, and Little 2018) etc. We also observe similar behavior in few of our experiments and we propose a new anomaly score metric based on the training data statistics to mitigate this issue.

While the aforementioned models are primarily handling OOD anomaly detection, methods like Ano-GAN (Schlegel et al. 2017) which uses adversarial training have shown promising results in the in-distribution anomaly detection

tasks. Ano-GAN is succeeded by a string of GAN-based methods (Zenati et al. 2018; Akçay, Atapour-Abarghouei, and Breckon 2018; Akçay, Atapour-Abarghouei, and Breckon 2019; Ngo et al. 2019), etc.

In this paper, we address both tasks of detecting in-distribution as well as out-of-distribution anomalies. To the best of our knowledge, we are the first to propose a unified model to address both of these tasks. We summarize the main contributions of our paper as follows:

- We propose **Adversarial Mirrored AutoEncoder (AMA)**, an AutoEncoder Discriminator style network where we use Mirrored Wasserstein loss in the discriminator to enforce better semantic-level reconstruction.
- We propose **Simplex Interpolation** in the latent space during training to improve model’s generalization.
- We introduce **Atypical Selection**, a Negative Selection style algorithm to sample and generate *synthetic negatives* and use them during training to improve the model’s performance.
- We propose a novel anomaly score metric that uses the training-data statistics along with reconstruction scores for better predictions.

Our method outperforms or matches recent Anomaly Detection methods on in-distribution anomaly detection on CIFAR-10 and MNIST datasets and on OOD anomaly detection on CIFAR-10 vs SVHN and Fashion MNIST vs MNIST datasets.

## Background and Related work

Anomaly detection has been studied in many forms, we are interested in two cases, in-distribution anomaly detection and out-of-distribution anomaly detection.

**In-Distribution anomaly detection with Deep Generative models** In general, we assume anomalies arise from a generative process that is different from that of normal samples. It does not have to be the case. What if one of the components of the generative process malfunctions and produces a faulty sample. Such cases come under in-distribution anomalies. This is a harder problem since anomalies are from the same-manifold and we should tune our anomaly detector to be sensitive to even such anomalies. Schlegl et al. (2017) is one of the early papers to adopt adversarial training for anomaly detection. They claim that the latent space of GAN represents the data distribution. It has been extended by Zenati et al. (2018) using BiGAN (Donahue, Krähenbühl, and Darrell 2016) to improve the latent representations of the data.

DeepSVDD (Ruff et al. 2018) is the deep learning implementation inspired by traditional SVDD (Support Vector Data Description) (Tax and Duin 2004) where a hypersphere is used to separate normal samples from anomalies. In DeepSVDD, an Encoder-Decoder network is used to learn the latent representations of the data while minimizing the volume of a lower-dimensional hypersphere that encloses them. They hypothesize that anomalous data is likely

to fall outside the sphere, and normal data is likely to fall inside the sphere.

**Out-of-Distribution detection with Deep NNs** Many of the current OOD methods are add-ons on top of discriminative classifiers trained on in-distribution data (Hendrycks and Gimpel 2016; Hendrycks, Mazeika, and Dietterich 2018; Liang, Li, and Srikant 2017). Generative models are sought after in the ood detection tasks since they work on completely unlabeled data, and the distribution can be modeled directly. To circumvent the issue of generative models assigning higher likelihoods to OOD samples, Ren et al. (2019) proposes to use the ratio of the likelihood of the model training on normal samples to the likelihood of the model training on random perturbations to this data. Higher the ratio less likely the sample is anomalous. Choi, Jang, and Alemi (2018) proposes to use the WAIC criterion on likelihood estimations from various independently trained models to recognize the OOD anomalies.

**Negative Selection Algorithms (NSA)** NSA is one of the early biologically inspired algorithms to solve one-class classification problem, first proposed by (Forrest et al. 1994) to detect data manipulation caused by computer viruses. The core idea is to find the detectors which do not match normal samples and use them for downstream tasks like anomaly detection (Dasgupta and Majumdar 2002), function optimization (Coello and Cortés 2002), etc. Gonzalez, Dasgupta, and Kozma (2002) first proposed to generate negative samples from unlabeled data and then train a classifier on the negatives and positive samples to learn the decision boundary. Since NSA-algorithms rely on too many detectors to understand the boundary of positive space, it can be quite complex computationally (Jinyin and Dongyong 2011). Recent work by Sipple (2020) proposes a simpler approach to perform Negative selection by using Uniform sampling and building a binary classifier with Positives and Synthetic Negatives to perform anomaly detection task.

## Problem Setup

In this paper, we consider the problem of identifying anomalies in a given dataset irrespective of their sources. Conventionally, anomalies are presumed to be generated by a different data distribution compared to that of the normal samples. For example, when we are dealing with CIFAR-10 images and an SVHN image is found in the mix, this would be an OOD anomaly. While in this example, there is a clear semantic shift, sometimes anomalies could just be inliers, i.e. they originate from the same manifold of the normal samples. For instance, when one class of CIFAR-10 is normal, rest 9 classes can be viewed as anomalous. For the sake of brevity, we use the same mathematical notation to refer to both in-distribution or out-of-distribution anomalies.

Let  $\{\mathbf{x}_1, \mathbf{x}_2, \dots, \mathbf{x}_m\} \sim \mathbb{P}_X$  be the set of normal samples available for training the model. Let  $\mathbb{Q}_X$  be the distribution generating the anomaly samples. Following the same setup as (Ruff et al. 2018; Zenati et al. 2018; Ren et al. 2019), we assume that all data in the training set are normal samples.

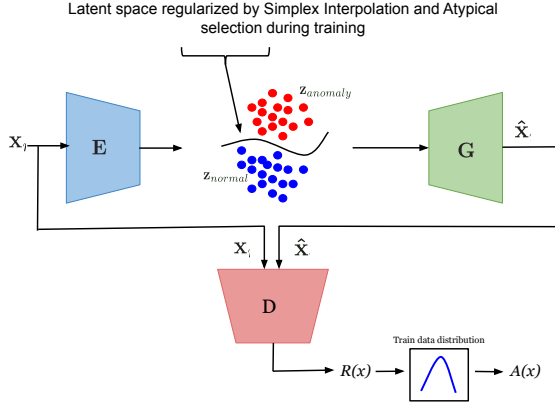


Figure 1: Anomaly detection pipeline: **E** is the Encoder, **G** is the Generator and **D** is the Discriminator. First we train the model on normal samples and synthetic negatives, sampled via Atypical Selection if enabled along with the simplex interpolation in latent space. This results in a rather smooth and compact latent manifold for the normal samples. During the test time, the discriminator network extracts the features representations of (input  $x$ , reconstruction  $\hat{x}$ ) pairs. These features are used to compute  $R(x)$  which is further used to compute  $A(x)$ , the likelihood of  $x$  being normal.

In appendix, we address the scenario in which the training data is corrupted with anomalies.

**Abbreviations** Going forward, by normal samples we mean samples which are non-anomalous, or desired samples. We are *not* referring to the Gaussian normal distribution. Also, we might use a shorthand AD for Anomaly detection, OOD for out-of-distribution, ID for in-distribution.

### Mirrored Adversarial Auto-Encoder

For auto-encoder training, usually  $L_1$  or  $L_2$  reconstruction loss between the original image and its reconstruction has been used, which can be define as  $\|x - x_{rec}\|_p$  where  $p = 1, 2$ . We propose to replace the pixel-level losses with a semantic-level reconstruction loss that is suited for the unsupervised anomaly detection.

$L_p$  reconstruction losses typically result in blurry reconstructions. Moreover, using  $L_p$  as an anomaly score provides poor estimates since  $L_p$  distances do not measure the semantic similarities between images. Additionally, a high  $L_p$  reconstruction loss between an input and its decoded image can be an outcome of a poor reconstruction quality and not because the image is in fact an anomaly. Our proposal is to replace the  $L_p$  reconstruction loss with a novel adversarial loss, which is motivated by the following reasons: (1) To improve the quality of reconstructions, (2) To use a discriminator to obtain a semantically meaningful measure of anomaly score.

In Fig. 1, we show an outline of our framework. We have a standard Auto-Encoder with 3 major improvements: (i) Mirrored Wasserstein Loss, (ii) Latent space Simplex Interpolation, and (iii) Atypical Selection. We will discuss these

components in the subsequent sections. Unlike an Adversarial AutoEncoder (Makhzani et al. 2015) which places the discriminator in the bottleneck, our model places the discriminator post the reconstruction step.

### Discriminator Design

For a given sample  $x$  and its reconstruction  $\hat{x}$ , we use a discriminator **D** to measure the Wasserstein distance between the joint distribution  $(x, x)$  and  $(x, \hat{x})$ . This approach differs from a conventional Wasserstein GAN-based architectures (Martin Arjovsky and Bottou 2017) as Wasserstein distance between the joint distribution of images and reconstructed images are minimized instead of the marginal distributions. We use this loss function because, for training AutoEncoders, we need to reconstruct a sample that looks similar to that of the input sample. Just minimizing the Wasserstein distance between marginals of real and reconstructed samples would result in a situation where an input and its generated sample both belong to the same distribution, yet semantically different. For example, a cat image in a CIFAR-10 dataset can be reconstructed as an airplane. This will still be a feasible solution since both airplane and cat belong to the same input distribution, hence the Wasserstein distance will be small.

To resolve this issue, we perform a Wasserstein minimization between the joint distributions  $\mathbb{P}_{X,X}$  and  $\mathbb{P}_{X,\hat{X}}$ . The discriminator now takes in stacked pairs of input images  $(x, x)$  and  $(x, \hat{x})$ . This clearly avoids the problems discussed in the previous part as the distribution  $(x, x)$  always has pairs of samples that are similar looking. If a car image is reconstructed as an airplane, the generated distribution will contain a (car, airplane) sample, which is never found in the input distribution  $(x, x)$ . Hence, the model will aim to generate samples sharing the same semantics. We would like to point out that the formulation presented here is equivalent to matching conditional distributions between  $W(\mathbb{P}_{X|X}, \mathbb{P}_{\hat{X}|X})$ . This model also shares similarities to discriminator architectures used in conditional image to image translations such as Pix2Pix (Isola et al. 2017).

Mathematically, our formulation can be written as:

$$W(\mathbb{P}_{X,X}, \mathbb{P}_{X,\hat{X}}) = \max_{D \in Lip-1} \mathbb{E}_{x \sim \mathbb{P}_X} [D(x, x) - D(x, \hat{x})] \quad (1)$$

where  $\hat{x} = G(E(x))$ .

**Lemma 1** *If  $E$  and  $G$  are optimal encoder and generator networks, i.e.,  $\mathbb{P}_{X,G(E(X))} = \mathbb{P}_{X,X}$ , then  $x = G(E(x))$ .*

### Latent Space Interpolation

Interpolation is a way to enhance the structure of the latent space in an autoencoder. By forcing intermediate points along the interpolation to be indistinguishable from real data distribution, (Berthelot et al. 2018) shows that the representation in latent space gets enhanced, leading to improved performance on downstream tasks such as supervised learning and clustering. However, Sainburg et al. (2018) argues that pairwise interpolation between samples of  $x$  proposed by Berthelot et al. (2018) do not reach all points within the

latent distribution, and may not necessarily make the latent distribution compact. Hence, we propose Simplex interpolation to make the manifold smoother and amenable. Given 3 normal samples  $\mathbf{x}_1, \mathbf{x}_2, \mathbf{x}_3$  and  $\alpha_i$ 's coefficients sampled uniformly from  $[0, 0.5]$ , we define:

$$\hat{\mathbf{x}}_{inter} = \mathbf{G}(\alpha_1 \mathbf{e}_1 + \alpha_2 \mathbf{e}_2 + (1 - \alpha_1 - \alpha_2) \mathbf{e}_3)$$

$$\mathbf{e}_i = \mathbf{E}(\mathbf{x}_i) \quad \forall i$$

A discriminator is then trained to distinguish between  $(\mathbf{x}, \mathbf{x})$  pair and  $(\mathbf{x}, \hat{\mathbf{x}}_{inter})$  pair, while the generator learns by trying to fool the discriminator. Note that the proposed simplex interpolation can be easily extended to  $m$  points by considering  $\alpha_i$ 's s.t.  $\sum_{i=1}^m \alpha_i = 1$  where  $\alpha_i \geq 0 \quad \forall i$ .

### Atypical Selection: Negative Sampling from Atypical Set

In our approach, we use feature representation from the discriminator network to obtain the anomaly scores (Fig. 1). To enhance this feature representation for anomaly detection, we use negative sampling (Sippl 2020) – a technique in which synthetic negatives are sampled in the latent space and are utilized for training an anomaly classifier. We propose a novel way to sample the synthetic negatives by using the concept of typical sets.

A typical set of a probability distribution is the set whose elements have information content close to that of the expected information. It is essentially the volume that not only covers most of mass of the distribution, but also reflects the properties of samples from the distribution. Due to the concentration of measure, a generative model will draw samples only from typical set (Cover 1999). Even though the typical set has the highest mass, it might not have the highest probability density. Recent works (Choi, Jang, and Alemi 2018; Nalisnick et al. 2019) propose that normal samples reside in typical set while anomalies reside outside of typical set, sometimes even in high probability density region. Hence we propose to sample outside the typical set in the latent space to generate synthetic negatives.

The Gaussian Annulus Theorem (Blum, Hopcroft, and Kannan 2016; Vershynin 2018) states that in a  $d$ -dimensional space, a typical set resides with high probability at a distance of  $\sqrt{d}$  from the origin. In the absence of true negatives, we can obtain synthetic negatives by sampling the latents just outside and closer to the typical set than the origin and then using the generator for reconstruction. Although, our latent space is not Gaussian, we observe that an L2 regularization ensures that representations of most of the positive samples are close to  $\sqrt{d}$  in magnitude. We sample for atypical points uniformly between spheres with radii  $\sqrt{d}$  and  $\sqrt{d} \pm \delta$  as illustrated in Fig. 2(b)(c). We call this procedure **Atypical Selection**. The  $\delta$  and the direction of the selection are hyperparameters which are chosen based on the true anomaly samples available during the validation time. Fig. 3 compares synthetic negatives to the normal reconstructions.

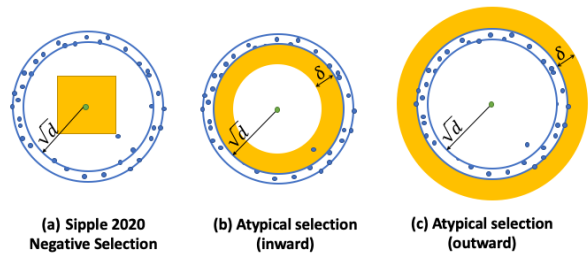


Figure 2: An illustration of the negative sampling from atypical set in the latent space. In each of the cases, typical set resides between the two blue  $d$ -dimensional spheres. Regions in which negative samples are generated are shown in yellow. (a) In (Sippl 2020), a cube centered at the origin is used as the negative sampling region. Instead, we propose to sample the synthetic negatives closer to the typical set between the spheres (b)  $\sqrt{d} - \delta$  and  $\sqrt{d}$  or (c)  $\sqrt{d}$  and  $\sqrt{d} + \delta$ .

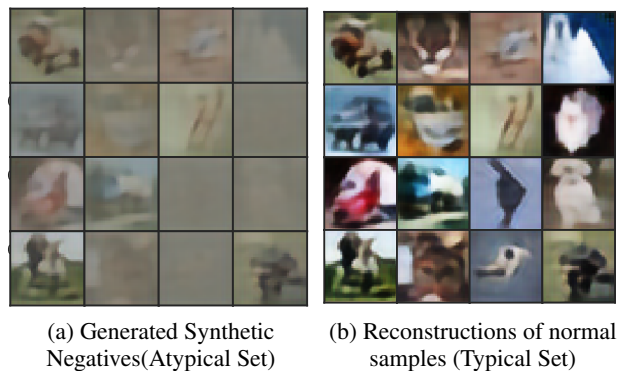


Figure 3: **Sample Generations:** Plot (a) shows samples generated by latents from the atypical set, while (b) shows samples generated by latents from the typical set. Negative samples clearly look different from clean CIFAR-10 samples.

### Overall Objective

Let  $\tilde{\mathbb{Q}}_X$  be the distribution of all atypical samples and let  $\mathbb{P}_X$  be the distribution of normal samples.

**Unsupervised case:** In this paper, we consider an unsupervised case where only normal samples are available in the training. Hence, we train the generative model using the following min-max objective:

$$\min_{\mathbf{G}} \max_{\mathbf{D} \in Lip-1} \mathcal{L}_{normal} - \lambda_{neg} \mathcal{L}_{neg} \quad (2)$$

$$\mathcal{L}_{normal} = \mathbb{E}_{\mathbf{x} \sim \mathbb{P}_X} [\mathbf{D}(\mathbf{x}, \mathbf{x}) - \mathbf{D}(\mathbf{x}, \hat{\mathbf{x}})] + \quad (3)$$

$$\lambda_{inter} [\mathbf{D}(\mathbf{x}, \mathbf{x}) - \mathbf{D}(\mathbf{x}, \hat{\mathbf{x}}_{inter})] + \quad (4)$$

$$\lambda_{reg} \|\mathbf{E}(\mathbf{x})\|$$

$$\mathcal{L}_{neg} = \mathbb{E}_{\mathbf{x} \sim \tilde{\mathbb{Q}}_X} [\mathbf{D}(\mathbf{x}, \mathbf{x}) - \mathbf{D}(\mathbf{x}, \hat{\mathbf{x}}_{neg})] \quad (5)$$

$\hat{\mathbf{x}}_{neg} = G(\mathbf{z}_{neg})$ , where  $\mathbf{z}_{neg}$  is the latent sampled by Atypical Selection.  $\lambda_{neg}$  is the Atypical Selection hyperparameter,

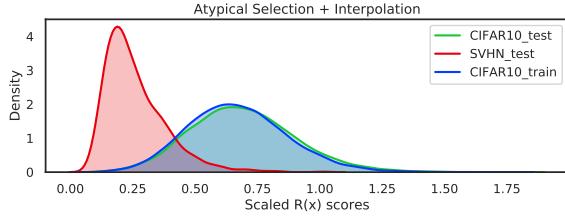


Figure 4: **OOD detection performance** when CIFAR-10 is the in-distribution dataset. We plot the density of anomaly scores  $R(x)$  for CIFAR-10 and SVHN samples. We observe that the CIFAR-10 training distribution (blue curve) and test distribution (green curve) highly overlap. Anomaly scores of SVHN samples (red curve), which is a OOD dataset, is much lower.

$\lambda_{inter}$  is the weight for the interpolation component,  $\lambda_{reg}$  is the latent space regularization weight and  $\|E(x)\|$  acts as regularizer for the latent representations.

**Semi-Supervised case:** If we have few real anomalies available during the training, we can easily extend this objective to such a case by using real anomalies instead of synthetic negatives in the  $\mathcal{L}_{neg}$  term. Please refer to appendix for some related experiments.

### Anomaly score

Previous methods (Schlegl et al. 2017; Ngo et al. 2019) used the discriminator output as an anomaly score. Zenati et al. (2018) proposed an improvement by computing the distance between a sample and its reconstruction in the feature space of the discriminator, which can be written as:

$$R(x) = \|f(x, x) - f(x, G(E(x)))\|_1 \quad (6)$$

where  $f(\cdot, \cdot)$  is the penultimate layer of the Discriminator  $\mathbf{D}$  and  $\mathbf{G}$  is the Generator and  $\mathbf{E}$  is the Encoder.

Zenati et al. (2018) claimed that the anomalous samples will have higher  $R(x)$  values compared to that of normal samples. While this is true for in-distribution anomalies, we observe a counter-intuitive behaviour in some OOD detection scenarios, similar to what Nalisnick et al. (2018); Choi, Jang, and Alemi (2018) reported for sample likelihoods. Our model assigns lower  $R(x)$  scores to OOD samples in the case of CIFAR-10 vs SVHN detection as shown in Fig. 4. Even though the  $R(x)$  distribution of test CIFAR-10 samples overlaps with training distribution quite well, if we use the  $R(x)$  scores to compute AUROC, it results in a very low AUC value, meaning most of the anomalies are classified as normals. Hence  $R(x)$  values account the absolute behavior of a sample, but not the relative behavior with respect to the training data. This suggests that this reconstruction-based score is not robust for all the scenarios.

Hence we propose: (i) fit the  $R(x)$  scores of training data to a Gaussian distribution (ii) compute the anomaly score for a given test sample  $x_i$  as the likelihood of  $R(x_i)$  under the Gaussian distribution. The proposed anomaly metric  $A(x_i)$

can be written as:

$$A(x_i) = \frac{1}{\sigma\sqrt{2\pi}} e^{-(R(x_i)-\mu)^2/2\sigma^2} \quad (7)$$

where  $\mu$  is the mean and  $\sigma^2$  is the variance of the distribution of  $R(x)$  over the training data.

Now with the new score  $A(x)$ , when we calculate the AUC score for the case presented in Fig. 4, it results in a value of 0.852, which truly captures the inherent behavior.

## Experiments

In this section we discuss the datasets, experiments and evaluation metrics on our method and other baselines.

**Datasets** Our model Adversarial Mirrored AutoEncoder (AMA) is agnostic to the origin of the anomaly. Hence we consider both the cases of in-distribution anomalies as well as OOD anomalies. Simply put, in-distribution anomalies arise from the same data manifold and OOD anomalies arise from different data manifold. For In-Distribution case, we have performed experiments on CIFAR and MNIST datasets. Following the setup from Ruff et al. (2018); Zenati et al. (2018), in each experiment we consider one class as normal and rest of the 9 classes as anomalies. As for the out-of-distribution detection experiments, we follow the same setting as in (Hendrycks and Gimpel 2016; Liang, Li, and Srikant 2017; Ren et al. 2019) and use CIFAR-10 as normals vs SVHN as anomalies. Also we use Fashion MNIST as normals vs MNIST as anomalies.

**Evaluation Metrics** We use the the following commonly used metrics in AD: the area under the ROC curve (AUROC), the area under the precision-recall curve (AUPRC), and the false positive rate at 80% true positive rate (FPR80).

**Baselines** Previous methods (Akçay, Atapour-Abarghouei, and Breckon 2019; Zenati et al. 2018; Schlegl et al. 2017; Ngo et al. 2019; Ruff et al. 2018) address only the case of in-distribution detection. And methods like (Ren et al. 2019; Choi, Jang, and Alemi 2018) address only OOD detection case. We compare our model against models from either of the scenarios. We have implemented DeepSVDD for the OOD anomaly detection case since it is the next best performing method for the in-distribution case.

In cases of SkipGanomaly and Fence-GAN, in the original paper, the experiments were conducted assuming one of the classes as anomalies and the rest of the classes as normals. In rest of the papers (Zenati et al. 2018; Ruff et al. 2018; Schlegl et al. 2017), the setup is viceversa where one class is considered normal and the rest as anomalies. To maintain the uniformity, we follow the latter setting and all the results shown in Table 1 are for this setting. In Fence-GAN, we have modified the loss function to fit the modified data setting. In DeepSVDD, Global Contrast Normalization is used on the data prior to the training. We removed this additional normalization step to make the method comparable to other baselines.

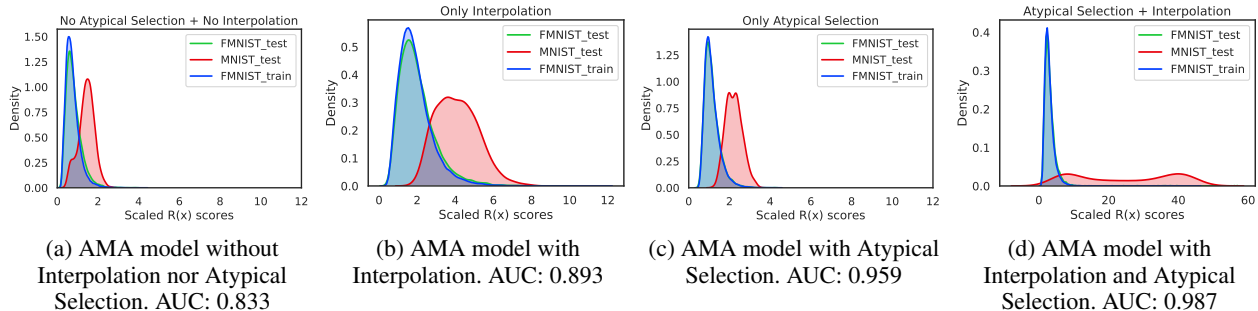


Figure 5: **OOD detection performance** with Fashion MNIST as the normal class and MNIST as the anomaly class. Each plot shows the histogram of anomaly scores using different components of AMA training. In each plot, blue and green curves represent the training and test distributions of the Fashion MNIST dataset, while the red curve represents the MNIST test distribution (OOD). We observe that both simplex interpolation and atypical selection help improve anomaly detection by shifting away the histogram of anomaly samples from the normal ones. Using both these techniques in combination yields the best results.

Class	0	1	2	3	4	5	6	7	8	9	Average
Fence GAN	0.754	0.307	0.628	0.566	0.390	0.490	0.538	0.313	0.645	0.408	0.504
ALAD	0.962	0.915	0.794	0.821	0.702	0.79	0.843	0.865	0.771	0.821	0.828
Ano-GAN	0.902	0.869	0.623	0.785	0.827	0.362	0.758	0.789	0.672	0.720	0.731
Skip-Ganomaly	0.297	0.877	0.393	0.486	0.618	0.540	0.455	0.633	0.426	0.584	0.531
Deep SVDD	0.971	0.995	0.809	0.884	<b>0.920</b>	0.869	0.978	0.940	<b>0.900</b>	0.946	0.921
AMA (Ours)	<b>0.986</b>	<b>0.998</b>	<b>0.882</b>	<b>0.891</b>	0.894	<b>0.938</b>	<b>0.981</b>	<b>0.983</b>	0.876	<b>0.948</b>	<b>0.938</b>

Class	airplane	automobile	bird	cat	deer	dog	frog	horse	ship	truck	Average
Fence GAN	0.572	0.582	0.505	0.544	0.534	0.535	0.528	0.537	0.664	0.338	0.567
ALAD	0.679	0.397	0.685	<b>0.652</b>	0.696	0.550	0.704	0.463	<b>0.787</b>	0.391	0.601
Ano-GAN	0.602	0.439	0.637	0.594	<b>0.755</b>	0.604	<b>0.730</b>	0.498	0.675	0.445	0.598
Skip-Ganomaly	0.655	0.406	0.663	0.598	0.739	0.617	0.638	0.519	0.746	0.387	0.597
Deep SVDD	0.682	0.477	0.679	0.573	0.752	0.628	0.710	0.511	0.733	0.567	0.631
AMA (Ours)	<b>0.752</b>	<b>0.634</b>	<b>0.696</b>	0.603	0.733	<b>0.650</b>	0.658	<b>0.582</b>	0.754	<b>0.632</b>	<b>0.669</b>

Table 1: Unsupervised Anomaly Detection performance on MNIST and CIFAR-10 datasets. Each column denotes the normal class and the rest 9 classes from that respective dataset are considered as anomalies. Performance reported are AUC scores (The higher, the better).

	Model	AUROC $\uparrow$	AUPRC $\uparrow$	FPR80 $\downarrow$
Case (a)	Deep-SVDD	0.864	0.812	0.213
	WAIC	0.221	0.401	0.911
	LikelihoodRatio	<b>0.994</b>	0.993	<b>0.001</b>
	AMA (Ours)	0.987	<b>0.999</b>	<b>0.001</b>
Case (b)	Deep-SVDD	0.171	0.975	0.219
	WAIC	0.146	0.343	0.956
	LikelihoodRatio	0.931	0.881	<b>0.066</b>
	AMA (Ours)	<b>0.935</b>	<b>0.992</b>	0.086

Table 2: (a) Evaluation metrics on Fashion MNIST (normal) vs MNIST (anomaly). (b) Evaluation metrics on CIFAR-10 (normal) vs SVHN (anomaly).

**BatchNorm** While we were working on the baselines, we noticed that one of the earlier work (Akçay, Atapour-Abarghouei, and Breckon 2019)<sup>1</sup> has evaluated their model in the training mode instead of setting it in the evaluation mode. This issue also affected the first version of this work.

<sup>1</sup><https://github.com/samet-akcay/skip-ganomaly>

Due to this issue, the BatchNorm is calculated for the test batch, rather than using the train-time statistics. While this might be acceptable for scenarios where we are evaluating and annotating the anomalies in batches, this is not a usual Anomaly Detection setting where we evaluate one sample at a time to check whether it is an anomaly or not. This will fail if (1) the evaluation is performed one example at a time, or if (2) the proportion of normal samples to anomalies is different during test as compared to training, which is usually the case in experimental setups of existing methods. Hence all the results reported in Table 1 are computed by freezing the BatchNorm statistics during the test time.

**Network Architectures and Training** The generator and the discriminator architectures are borrowed from Spectral Normalization GAN (Miyato et al. 2018). Our Encoder is a 4 layered convolution network with BatchNorm and LeakyRelu nonlinearity. The whole pipe-line is trained end-to-end with stochastic gradient descent with Nesterov momentum. Refer to appendix for the complete architecture de-

tails.

The validation dataset is approximately 1.5% the size of the training data. We assume we have access to few anomalies during validation time (100 normals and 10 anomalies in ID case, 500 normals and 50 anomalies in OOD case) similar to the setting in (Zenati et al. 2018; Ren et al. 2019) to choose the best performing model. We have taken the default test data of CIFAR-10/MNIST as test data for in-distribution AD experiments. For OOD experiments, we randomly select 1000 (10% the size of normal test samples) anomalies from the corresponding anomaly dataset and add it to the normal data testset (for example in CIFAR-10 vs SVHN case, along with the 10000 CIFAR-10 test images, we randomly select 1000 samples from SVHN).

We keep the test data and normalizations same for our model as well as the baselines to make them comparable. We trained each model for 100 epochs with a batchsize of 256 for all the datasets with a learning rate starting of  $3e-4$  and decaying it by a factor of 0.1 at 30%, 60% and 90% of the training epochs. During training we run the model for first 10 epochs only on normal samples, from 11<sup>th</sup> epoch onwards we generate synthetic anomalies and use them along with normal samples in training. We use  $\lambda_{interp} = 0.5$ ,  $\lambda_{neg} = 5$  and  $\lambda_{reg} = 1$  in all of our CIFAR-10 experiments. Refer to the appendix for the hyperparameter values of MNIST experiments. In OOD experiments, for CIFAR-10, we sampled for synthetic anomalies towards the origin and for the Fashion MNIST case we sampled outward. Experiments are performed using two NVIDIA GTX-2080TI GPUs.

## Results

We believe ours is the first model to achieve competitive performance for both in-distribution and OOD Anomaly Detection scenarios simultaneously.

**In-distribution anomaly detection** We present the results of our in-distribution Anomaly Detection experiments in Table 1. We present the AUROC scores on both MNIST and CIFAR-10. Each column shows the results of a normal class with the rest of 9 classes as anomalies. Our method (AMA) outperforms other methods in terms of average scores with 1.7% AUC gain over the next best method on MNIST and 3.7% gain on CIFAR-10 dataset. In terms of an individual case comparison, we best 8 out of 10 cases on MNIST, while 6 out of 10 cases on CIFAR-10.

While most of the methods fail in classes like automobile and truck, our method is performing relatively well. We can attribute this improvement to the Interpolation and Atypical Selection as shown in Figure 6 (top). Since the resolution of images is low, some images are hard to tell apart even for humans. For example, some dog images look like cats even for humans. So in the experiment where cat is a normal class and rest 9 classes anomalous, our model is classifying few of the dog images as cats, leading to lower AUC scores. The same trend follows for other similar-looking classes, like deer vs horse, ship vs airplane etc. Another observation is, our anomaly metric heavily relies on the similarity of test and train distributions. If there is a non-semantic distributional shift in test data, AUC scores reduce and the model

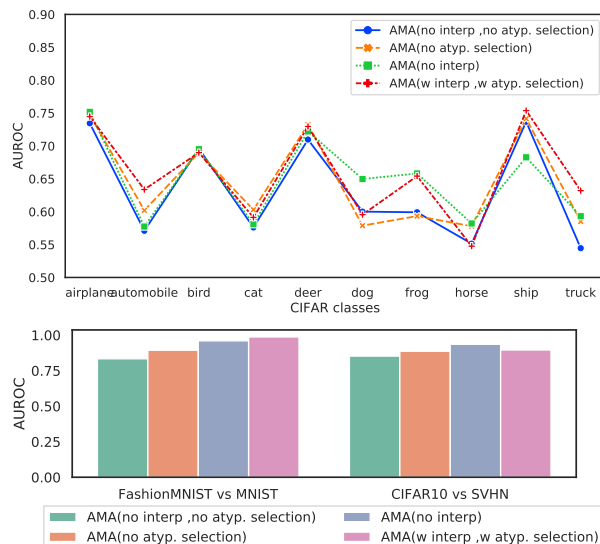


Figure 6: **Ablation analysis** on the use of simplex interpolation and atypical selection. The plot on the top panel shows anomaly detection when one class of CIFAR-10 is used as normal class, while the other 9 classes are used as anomalies. The plot on the bottom shows OOD detection when Fashion MNIST and CIFAR-10 are used as in-distribution datasets, respectively. We observe that both simplex interpolation and atypical selection improve performance, and using both components in combination yields the best results.

will tag such normal samples as anomalies, like we have observed in the case of the frog class.

Another interesting observation is, on our method, the classes which are more homogeneous perform better. For example, in the airplane class, the variance within data is much smaller compared to other classes like frog with close-up shots as well as distant shots with green, brown backgrounds, etc. In the former case, interpolation strongly boosts the performance of the model while it can hurt it in the latter case (see Fig. 6 (top)). Please refer to the appendix for other supporting plots and further analysis.

**Out-of-distribution Anomaly detection** We present results of two cases of OOD Anomaly Detection experiments in Table 2. Our method (AMA) outperforms other baselines in CIFAR vs SVHN case, but in Fashion MNIST vs MNIST case, our numbers are very close to the best method, LLR, off by just 1%. Our method still has the best AUPRC performance in both of the scenarios. In addition to this, when we checked how our model generalizes to other datasets which the model has not seen before nor is tuned for, the performance of our model is impressive: In CIFAR-10 vs LSUN (as OOD) case, we have an AUC of 0.961, in CIFAR-10 vs iSUN (as OOD) we get an AUC of 0.935 and in CIFAR-10 vs Imagenet (as OOD) we obtain an AUC of 0.927 (In all 3 cases, the OOD images are resized, not cropped). This shows the model is optimizing the latent space of normal samples well which leads to an impressive generalization behavior.

**Ablation studies** The objective function of AMA consists of primarily 3 components: Mirrored Wasserstein loss, Simplex Interpolation and Atypical Selection. We analysed how much each component is contributing to the performance of the method by considering the following 4 cases. (i) Base AMA model without interpolation nor atypical selection (ii) AMA model with interpolation (iii) AMA model with atypical selection (iv) AMA model with both interpolation and atypical selection. We present ablation scenarios for each class of CIFAR-10 dataset in Figure 6(top). In Fig. 6 (bottom), we present the results on OOD scenarios. As you can see for most of the classes, all the components are contributing, some more than others in few cases. Fig. 5 gives us an intuition of how the  $R(x)$  scores are changing with each of the components.

## Conclusion

In this paper, we have presented a novel Anomaly Detection model, Adversarial Mirrored Autoencoder (AMA), which outperforms existing Anomaly Detection models. We introduced the Mirrored Wasserstein Loss, coupled with Simplex Interpolation and Atypical Selection in the training to improve the latent space representation of normal data. We show how each of the components contribute to the model's performance and how they work on diverse data settings. In the main text, we primarily discuss the unsupervised case, while the preliminary results for the semi-supervised case is discussed in the appendix.

## Acknowledgements

This project was supported in part by NSF CAREER AWARD 1942230, an IBM faculty award, a grant from Capital One, and a Simons Fellowship on Deep Learning Foundations. This work was supported through the IBM Global University Program Awards initiative. Authors thank Ritesh Soni, Steven Loscalzo, Bayan Bruss, Samuel Sharpe and Jason Wittenbach for helpful discussions.

## References

- Akçay, S.; Atapour-Abarghouei, A.; and Breckon, T. P. 2018. Ganomaly: Semi-supervised anomaly detection via adversarial training. In *Asian conference on computer vision*, 622–637. Springer.
- Akçay, S.; Atapour-Abarghouei, A.; and Breckon, T. P. 2019. Skip-ganomaly: Skip connected and adversarially trained encoder-decoder anomaly detection. In *2019 International Joint Conference on Neural Networks (IJCNN)*, 1–8. IEEE.
- Amodei, D.; Olah, C.; Steinhardt, J.; Christiano, P.; Schulman, J.; and Mané, D. 2016. Concrete problems in AI safety. *arXiv preprint arXiv:1606.06565*.
- Berthelot, D.; Raffel, C.; Roy, A.; and Goodfellow, I. 2018. Understanding and improving interpolation in autoencoders via an adversarial regularizer. *arXiv preprint arXiv:1807.07543*.
- Blum, A.; Hopcroft, J.; and Kannan, R. 2016. Foundations of data science. *Vorabversion eines Lehrbuchs* 5.
- Chalapathy, R.; and Chawla, S. 2019. Deep learning for anomaly detection: A survey. *arXiv preprint arXiv:1901.03407*.
- Chandola, V.; Banerjee, A.; and Kumar, V. 2009. Anomaly detection: A survey. *ACM computing surveys (CSUR)* 41(3): 1–58.
- Choi, H.; Jang, E.; and Alemi, A. A. 2018. Waic, but why? generative ensembles for robust anomaly detection. *arXiv preprint arXiv:1810.01392*.
- Coello, C. A. C.; and Cortés, N. C. 2002. An approach to solve multiobjective optimization problems based on an artificial immune system.
- Cover, T. M. 1999. *Elements of information theory*. John Wiley & Sons.
- Dasgupta, D.; and Majumdar, N. S. 2002. Anomaly detection in multidimensional data using negative selection algorithm. In *Proceedings of the 2002 Congress on Evolutionary Computation. CEC'02 (Cat. No. 02TH8600)*, volume 2, 1039–1044. IEEE.
- Donahue, J.; Krähenbühl, P.; and Darrell, T. 2016. Adversarial feature learning. *arXiv preprint arXiv:1605.09782*.
- Forrest, S.; Perelson, A. S.; Allen, L.; and Cherukuri, R. 1994. Self-nonsel self discrimination in a computer. In *Proceedings of 1994 IEEE computer society symposium on research in security and privacy*, 202–212. Ieee.
- Gonzalez, F.; Dasgupta, D.; and Kozma, R. 2002. Combining negative selection and classification techniques for anomaly detection. In *Proceedings of the 2002 Congress on Evolutionary Computation. CEC'02 (Cat. No. 02TH8600)*, volume 1, 705–710. IEEE.
- Gulrajani, I.; Ahmed, F.; Arjovsky, M.; Dumoulin, V.; and Courville, A. C. 2017. Improved training of wasserstein gans. In *Advances in neural information processing systems*, 5767–5777.
- Hendrycks, D.; and Gimpel, K. 2016. A baseline for detecting misclassified and out-of-distribution examples in neural networks. *arXiv preprint arXiv:1610.02136*.
- Hendrycks, D.; Mazeika, M.; and Dietterich, T. 2018. Deep anomaly detection with outlier exposure. *arXiv preprint arXiv:1812.04606*.
- Hsu, Y.-C.; Shen, Y.; Jin, H.; and Kira, Z. 2020. Generalized odin: Detecting out-of-distribution image without learning from out-of-distribution data. In *Proceedings of the IEEE/CVF Conference on Computer Vision and Pattern Recognition*, 10951–10960.
- Isola, P.; Zhu, J.-Y.; Zhou, T.; and Efros, A. A. 2017. Image-to-image translation with conditional adversarial networks. In *Proceedings of the IEEE conference on computer vision and pattern recognition*, 1125–1134.
- Jinyin, C.; and Dongyong, Y. 2011. A study of detector generation algorithms based on artificial immune in intrusion detection system. In *2011 3rd International Conference on Computer Research and Development*, volume 1, 4–8. IEEE.

- Lee, K.; Lee, K.; Lee, H.; and Shin, J. 2018. A simple unified framework for detecting out-of-distribution samples and adversarial attacks. In *Advances in Neural Information Processing Systems*, 7167–7177.
- Liang, S.; Li, Y.; and Srikant, R. 2017. Enhancing the reliability of out-of-distribution image detection in neural networks. *arXiv preprint arXiv:1706.02690*.
- Makhzani, A.; Shlens, J.; Jaitly, N.; Goodfellow, I.; and Frey, B. 2015. Adversarial autoencoders. *arXiv preprint arXiv:1511.05644*.
- Martin Arjovsky, S.; and Bottou, L. 2017. Wasserstein generative adversarial networks. In *Proceedings of the 34th International Conference on Machine Learning, Sydney, Australia*.
- Miyato, T.; Kataoka, T.; Koyama, M.; and Yoshida, Y. 2018. Spectral normalization for generative adversarial networks. *arXiv preprint arXiv:1802.05957*.
- Nalisnick, E.; Matsukawa, A.; Teh, Y. W.; Gorur, D.; and Lakshminarayanan, B. 2018. Do deep generative models know what they don't know? *arXiv preprint arXiv:1810.09136*.
- Nalisnick, E.; Matsukawa, A.; Teh, Y. W.; and Lakshminarayanan, B. 2019. Detecting Out-of-Distribution Inputs to Deep Generative Models Using Typicality. *arXiv preprint arXiv:1906.02994*.
- Ngo, P. C.; Winarto, A. A.; Kou, C. K. L.; Park, S.; Akram, F.; and Lee, H. K. 2019. Fence GAN: towards better anomaly detection. In *2019 IEEE 31st International Conference on Tools with Artificial Intelligence (ICTAI)*, 141–148. IEEE.
- Ren, J.; Liu, P. J.; Fertig, E.; Snoek, J.; Poplin, R.; Depristo, M.; Dillon, J.; and Lakshminarayanan, B. 2019. Likelihood ratios for out-of-distribution detection. In *Advances in Neural Information Processing Systems*, 14707–14718.
- Ruff, L.; Vandermeulen, R.; Goernitz, N.; Deecke, L.; Siddiqui, S. A.; Binder, A.; Müller, E.; and Kloft, M. 2018. Deep one-class classification. In *International conference on machine learning*, 4393–4402.
- Sainburg, T.; Thielk, M.; Theilman, B.; Migliori, B.; and Gentner, T. 2018. Generative adversarial interpolative autoencoding: adversarial training on latent space interpolations encourage convex latent distributions. *arXiv preprint arXiv:1807.06650*.
- Schlegl, T.; Seeböck, P.; Waldstein, S. M.; Schmidt-Erfurth, U.; and Langs, G. 2017. Unsupervised anomaly detection with generative adversarial networks to guide marker discovery. In *International conference on information processing in medical imaging*, 146–157. Springer.
- Shafaei, A.; Schmidt, M.; and Little, J. J. 2018. A less biased evaluation of out-of-distribution sample detectors. *arXiv preprint arXiv:1809.04729*.
- Sipple, J. 2020. Interpretable, Multidimensional, Multimodal Anomaly Detection with Negative Sampling for Detection of Device Failure. *arXiv preprint arXiv:2007.10088*.
- Tax, D. M.; and Duin, R. P. 2004. Support vector data description. *Machine learning* 54(1): 45–66.
- Vershynin, R. 2018. *High-dimensional probability: An introduction with applications in data science*, volume 47. Cambridge university press.
- Vyas, A.; Jammalamadaka, N.; Zhu, X.; Das, D.; Kaul, B.; and Willke, T. L. 2018. Out-of-distribution detection using an ensemble of self supervised leave-out classifiers. In *Proceedings of the European Conference on Computer Vision (ECCV)*, 550–564.
- Zenati, H.; Romain, M.; Foo, C.-S.; Lecouat, B.; and Chandrasekhar, V. 2018. Adversarially learned anomaly detection. In *2018 IEEE International Conference on Data Mining (ICDM)*, 727–736. IEEE.
- Zhang, H.; Cisse, M.; Dauphin, Y. N.; and Lopez-Paz, D. 2017. mixup: Beyond empirical risk minimization. *arXiv preprint arXiv:1710.09412*.

# Appendix

## Proof of Lemma 1

**Lemma 2** If  $E$  and  $G$  are optimal encoder and generator networks, i.e.,  $\mathbb{P}_{X, \mathbf{G}(E(X))} = \mathbb{P}_{X, X}$ , then  $\mathbf{x} = \mathbf{G}(E(\mathbf{x}))$

**Proof:**

$$\begin{aligned} \mathbb{P}_{X, \hat{X}} &= \mathbb{P}_{X, X} \\ p(\hat{x} = k) &= \int_x p(x, \hat{x} = k) dx \\ &= p(x = k, \hat{x} = k) \end{aligned}$$

Therefore  $p(\hat{x} = k)$  is meaningful only if when  $\hat{x} = x$ , which means  $\mathbf{G}(E(x)) = x$ .

## Architectures

We present the complete architecture information of Adversarial Mirrored AutoEncoder (AMA) for CIFAR-10 and MNIST datasets for both in-distribution and OOD anomaly detection experiments in Table-3 and Table-4 respectively. We have used Spectral GAN elements in only CIFAR-10 experiments where in the discriminator  $\mathbf{D}$ , the BatchNorm is replaced by the Spectral Norm similar to SN-GAN’s architecture (Miyato et al. 2018).

## Atypical Selection vs Negative Sampling

In this section, we compare the performance of Atypical Selection against Negative Sampling proposed in Sipple (2020). We present the results in Table 5. We wanted to compare these two techniques with and without Simplex Interpolation in AMA. And we have analysed the performance in two OOD detection experiments, CIFAR-10 (normal) vs SVHN (anomalies) and Fashion MNIST (normal) vs MNIST (anomalies). Atypical Selection outperforms Sipple (2020)’s Negative Sampling in all 4 cases. The model’s performance is significantly better with Atypical selection in the Fashion MNIST vs MNIST case. This can be attributed to the outward Atypical Selection (Main paper Figure 2(c)) we used in this experiment, while Sipple (2020) always samples for anomalies inward and closer to the origin.

Regardless of presence of Simple Interpolation during training, Atypical selection model is performing better. We hypothesize that, since Atypical Selection technique samples near the boundary, it enforces the encoder to create more compact latent space for normal samples.

## Simplex Interpolation vs MixUp

We wanted to check if the Simplex Interpolation is contributing to the model any more than the general augmentation. MixUp (Zhang et al. 2017) is a famous augmentation technique based on interpolation in image space. So we have performed a comparative analysis of AMA model with either of Simplex Interpolation or MixUp as shown in Fig. 7. We have performed in-distribution Anomaly Detection experiments on CIFAR-10 considering one class as normal and

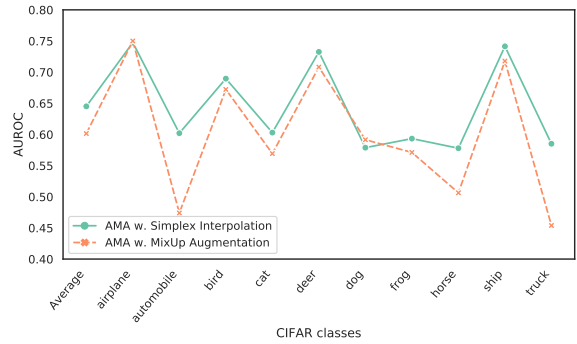


Figure 7: **Comparative analysis - Simplex Interpolation vs MixUp augmentation** when either of them are used in AMA during training. The experiments are performed on CIFAR-10 dataset with respective class on X-axis considered normal while rest of the 9 classes considered anomalous. We observe that Simplex Interpolation in training leads to a better model than using MixUp augmentation. The performance is reported in AUC scores, higher the better.

rest 9 as anomalous. Except for 2 classes, AMA with Simplex Interpolation outperformed AMA with MixUp in rest of the 8 classes. On average, AMA with Simplex Interpolation model has 4% AUC absolute gain over AMA with Mixup.

## Additional Results

**Corruption** One of the primary assumptions we made in our problem setup is, the training data consists of only normal samples. It is not a very realistic assumption since anomalies get stowed away as normal samples sometimes. We checked how our model performance gets affected when a few anomalies masked as normals (corruptions) are mixed in during the training time. We present the results of experiments at different levels of corruptions in Fig. 8. Let’s consider case of ‘dog’ as normal class with 5% corruption, in this experiment, in training we will have 5000 images of ‘dog’ class with 250 images randomly sampled from rest of the 9 classes and are marked normal. As the level of corruption increases, intuitively the AUC scores are dropping, but the performance drop is not quite drastic, between 0 and 10% corruption, the average AUC drops by 4.6% in absolute. But anomalies, by definition should be sparse, so 10% corruption model can be considered as the lower bound of our model’s performance.

**Misclassified** In Fig. 13 and Fig. 14, we show the misclassified images from both normal and anomaly data distribution. The False Negatives from both of the experiments seem to have sharp changes across the pixels, like dotted pattern frogs in CIFAR-10 case, and clothes with patterns in Fashion MNIST case. While in case of False positives in Fashion MNIST vs MNIST case are mostly 1’s and 7’s which resemble ‘pants’ category of Fashion MNIST data. One interesting observation is False Negatives in Fashion MNIST dataset are very similar to the low likelihood ratio images suggested by LLR method (Ren et al. 2019), which suggests

Generator	Encoder	Discriminator
$z \in \mathbb{R}^{128}$	$x \in \mathbb{R}^{32 \times 32 \times 3}$	$(x, \hat{x}) \in \mathbb{R}^{32 \times 32 \times 6}$
Dense, 4*4*256	((4,4),2,1,64)	ResBlock down 128
ResBlock up 256	BN + LeakyReLU(0.2)	ResBlock down 128
ResBlock up 256	((4,4),2,1,128)	ResBlock 128
ResBlock up 256	BN + LeakyReLU(0.2)	ResBlock 128
BN,ReLU,3 × 3 Conv, Tanh	((4,4),2,1,256)	ReLU
Adam( $\beta_1=0, \beta_2=0.999$ )	BN + LeakyReLU(0.2)	Global sum pooling
	((4,4),1,0,128)	dense → 1
	Adam( $\beta_1=0.5, \beta_2=0.999$ )	Adam( $\beta_1=0, \beta_2=0.999$ )

LR = 3e-4, Batch Size = 256, Epoch=100,  $\lambda_{inter} = 0.5$ ,  $\lambda_{neg} = 5$ ,  $\lambda_{reg} = 1$  and  $\delta = 0.5$ . Atypical Selection done inward.

Table 3: CIFAR-10 Architecture Detail. We use architecture from Miyato et al. (2018) and Gulrajani et al. (2017), Encoder Structure is represented as (filter\_size, stride, padding, output\_channel). The input to the discriminator is  $(x, x)$  or  $(x, \hat{x})$ , where images are stacked on the channel dimension.  $\hat{x}$  is the reconstruction of  $x$ .

Generator	Encoder	Discriminator
$z \in \mathbb{R}^{64}$	$x \in \mathbb{R}^{28 \times 28 \times 1}$	$(x, \hat{x}) \in \mathbb{R}^{28 \times 28 \times 2}$
Linear(64,1024)+ReLU	Conv((4,4),2,2,64) + RELU	Conv((4,4),2,2,64) +
Linear(1024,7*7*128)	Conv((4,4),2,2,128) + RELU	LeakyReLU(0.2)
+ReLU	Dense(1024) + RELU	Conv((4,4),2,2,128) +
ConvTranspose2d(4,4),2,2,64 +	Dense(64)	LeakyReLU(0.2)
RELU		Dense(1024) + LeakyReLU(0.2)
ConvTranspose2d(4,4),2,2,1 +		Dense(1)
Tanh		

LR = 3e-4, Batch Size = 256, Epoch=100,  $\lambda_{inter} = 0.5$ ,  $\lambda_{neg} = 5$ ,  $\lambda_{reg} = 1$  and  $\delta = 0.5$ . Atypical Selection done outward.

Table 4: MNIST Architecture Detail, for both in-distribution as well as OOD Anomaly Detection experiments.

	Experiment	Sipple 2020	Atypical Selection (Ours)
(a)	No interpolation	0.778	<b>0.960</b>
	With interpolation	0.824	<b>0.987</b>
(b)	No interpolation	0.852	<b>0.935</b>
	With interpolation	0.819	<b>0.895</b>

Table 5: Comparison table evaluating Sipple 2020 style negative sampling vs Atypical selection proposed by us. We have conducted experiments in presence and absence of Simplex Interpolation during training. The performance reported in the table are AUC scores. Higher the better (a) Evaluation on Fashion MNIST(normal) vs MNIST(anomaly) dataset. (b) Evaluation on CIFAR-10(normal) vs SVHN(anomaly) dataset.

that our anomaly metric might be in a way be related to LLR metric.

**How does the reconstructions look like?** We show how our model is reconstructing the samples in Fig. 10. It is interesting that our model does not reconstruct the anomalies well in some experiments, so while using our model, it is possible to qualitatively tell apart which images are normals and which ones are anomalies just by comparing an image to its reconstruction.

**How does the interpolations look like?** In Figures 11,12, we show how the interpolated latent representations look like compared to interpolations in image space. It is very visible in Fashion MNIST case, the latent interpolations are

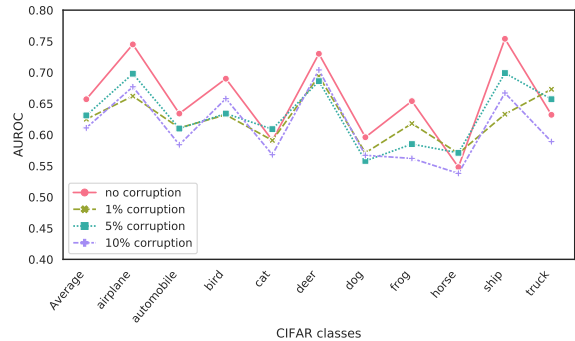


Figure 8: **Comparative analysis** of when corruptions (anomalies masked as normals) are introduced in training. Each experiment considers the class(on X-axis) as normal data and rest 9 as anomalous data. Performance is measured as AUC scores, higher the better. Despite corruption, performance drop is not too high. All the experiments are conducted with same hyper-parameters.

generating semantically meaningful images as we interpolate between two points in test data set.

**Misc.** In Fig. 9, we present the ablation results in MNIST in-distribution anomaly detection experiment by turning off Atypical Selection or Simplex Interpolation or both.

### Semi-supervised training

One of the main advantages of our model is, it is easily extendable to Semi-supervised scenario. What we mean by

Anom %	airplane	automobile	bird	cat	deer	dog	frog	horse	ship	truck	Average
0	0.752	0.634	0.696	0.603	0.733	0.650	0.658	0.582	0.754	0.632	0.669
0.1	0.776	0.582	0.699	0.556	0.743	0.599	0.723	0.553	0.781	0.473	0.648
1	0.809	0.732	0.729	0.613	0.749	0.667	0.759	0.716	0.834	0.665	0.727
5	0.847	0.814	0.744	0.747	0.788	0.741	0.827	0.784	0.873	0.798	0.796
10	0.870	0.892	0.775	0.760	0.823	0.810	0.855	0.851	0.887	0.831	0.835
20	0.870	0.910	0.814	0.785	0.813	0.832	0.859	0.879	0.895	0.867	0.852

Table 6: Semi-supervised Anomaly Detection performance on CIFAR-10 dataset. Each column denotes the normal class and the rest 9 classes from CIFAR-10 are considered as anomalies. Each row represents the case where a certain percentage of anomalies are available during training. Performance reported are AUC scores. (Higher the better)

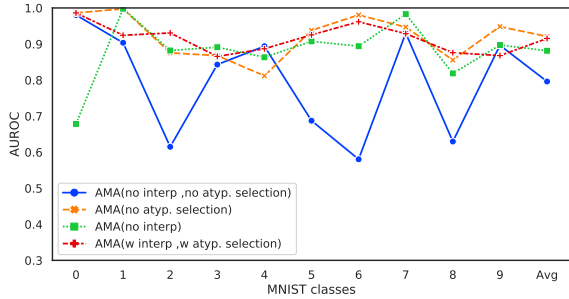


Figure 9: **Ablation analysis** on the use of simplex interpolation and atypical selection. The plot shows anomaly detection when one class of MNIST is used as normal class, while the other 9 classes are used as anomalies. We observe that both simplex interpolation and atypical selection improve performance, and using both components in combination yields the best results.

semi-supervised setting here is, a few tagged anomalies are available to us during train time along with many normal samples. We can use the objective from Equation (2) in the main paper and use real anomalies instead of atypical selected anomalies.

In Table 6, we present the results of various cases of training setting. The first column shows the ratio of anomalies available during training time to the number of normal samples available in training. And each column represents the case where that particular class is considered normal and rest of the 9 classes are considered anomalous. For eg, in 1% anomalies in training for dog experiment has - 5000 dog samples (normal), and 50 images randomly chosen for rest of the 9 classes (anomalies) are available during the training time. We can infer from the table, as the percentage of anomalies available during training increases, the model performance increases.

One interesting case is when we have 0.1% of real anomalies available during the training. While in few classes like airplane;ship, using real anomalies certainly improves the performance compared to 0% real anomalies case, it did not improve in rest of the classes. This could be attributed to the extremely small size of real anomalies set (5 in this case). Hence in scenarios where very few real anomalies are available, we can improve the model by coupling real anomalies with some atypical sampled anomalies.

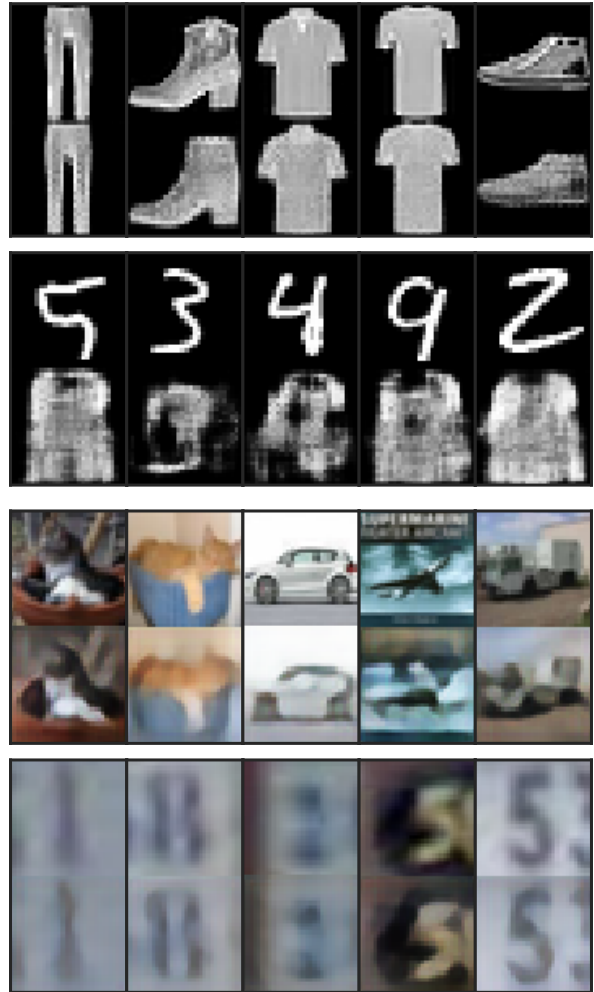


Figure 10: **Reconstructions** of normal and anomalous samples in OOD Anomaly Detection experiments. Odd rows represent the true images, and the even rows show the reconstructions. In the top panel, we have Fashion MNIST vs MNIST results, and in the bottom part, we have CIFAR-10 vs SVHN results.

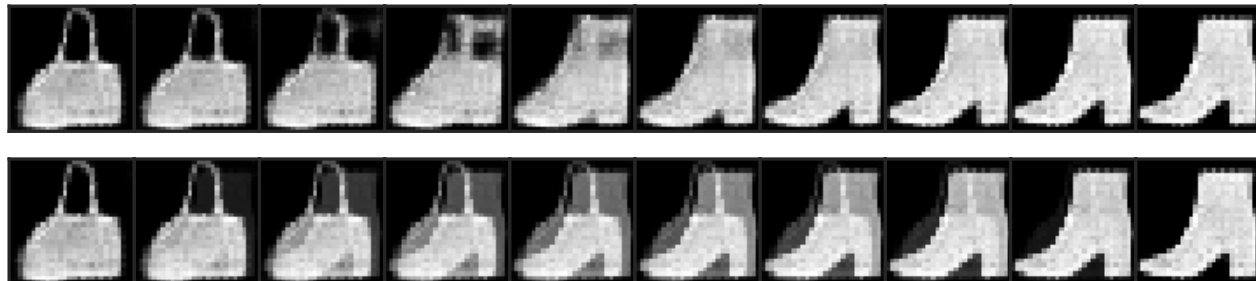


Figure 11: **Interpolations** of Fashion MNIST images in latent and image spaces. Top panel shows how the reconstructions of interpolations in latent space. Bottom panel shows results when images are interpolated in image space. Clearly the latent interpolations look much better. The first and last images are from Fashion MNIST dataset in each row.

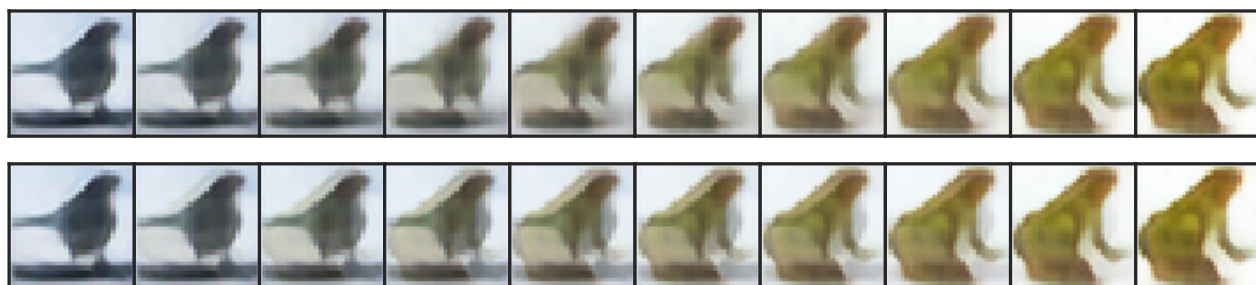


Figure 12: **Interpolations** of CIFAR-10 images. Similar to Fig. 11, the top panels shows interpolation in latent space, while bottom panels shows interpolation in image space.

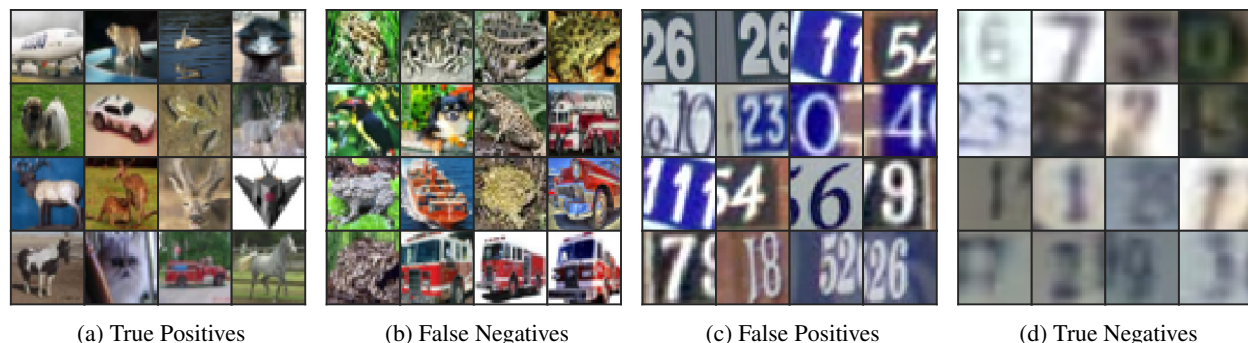


Figure 13: We show here the plots with highest and lowest  $A(x)$  (Main paper - equation 7) from both CIFAR-10 (normal) and SVHN (anomaly) classes. (a) True positives are from Normal class and have high  $A(x)$  scores (b) False Negatives are from Normal class and have low  $A(x)$  scores (c) False Positives are from Anomaly class and have high  $A(x)$  scores. (d) True Negatives are from Anomaly class and have low  $A(x)$  scores.

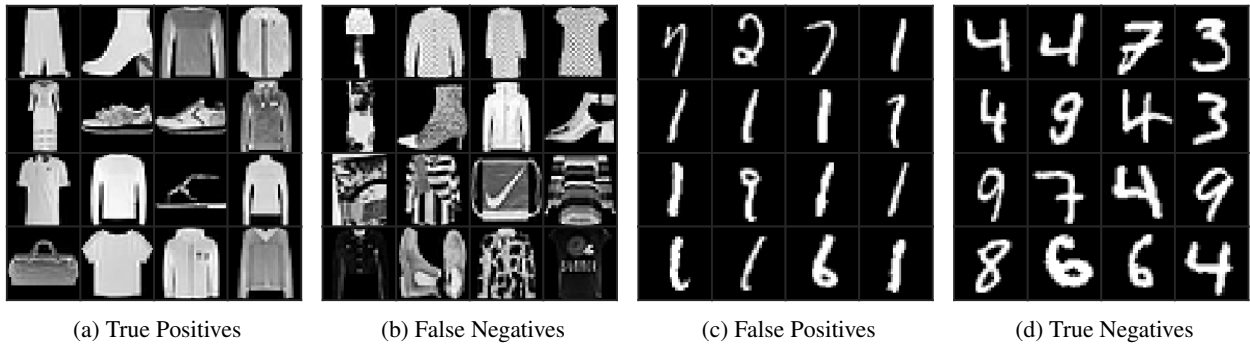


Figure 14: Similar to Fig. 13, here we show the plots with highest and lowest  $A(x)$  (Main paper - equation 7) from Fashion MNIST (normal) and MNIST (anomaly) classes. (a) True positives are from Normal class and have high  $A(x)$  scores (b) False Negatives are from Normal class and have low  $A(x)$  scores (c) False Positives are from Anomaly class and have high  $A(x)$  scores. (d) True Negatives are from Anomaly class and have low  $A(x)$  scores.